

Triax Accelerometer for Route-Based Vibration Analysis

A newly-developed triax accelerometer developed specifically for route-based vibration data acquisition for industrial machinery condition monitoring is presented. The sensor incorporates a two pole (two feet) integral magnet such that it can be placed on a curved surface. When the newly-developed triax sensor is mounted on the curved surface of a machine, the bandwidths of all three sensors are sufficient to capture the mechanical vibration and limited stress wave activity. If the sensor is placed on a flat surface (mounting pad), the bandwidth of the Z axis is sufficient to capture the stress wave activity accompanying impacting, fatiguing and friction. Assuming a two channel data collector is employed, simultaneous two channel data acquisition can be executed such as Z-axis mechanical vibration paired with Z-axis stress wave analysis followed by X-axis paired with Y-axis mechanical vibration resulting in significant time savings.

The triax sensor was demonstrated to reach all design goals in the laboratory. Data has been acquired in the field with the triax sensor in the normal route mode of data acquisition and shown to be essentially the same as the same data acquired employing the single axis sensor. The field experience has verified a time saving around 30%.

Introduction

When collecting vibration data for condition monitoring of industrial machinery in a route based (portable) mode, the most common sensor employed is a single axis accelerometer mounted to a 2-pole (two feet) magnet. The magnet is easily attached to a curved surface (providing two line contact) thereby requiring a minimal surface preparation at the measurement point. Experience has shown this means of collecting vibration data provides meaningful results for the detection and trending of many mechanical faults experienced in the industrial environment.

It is desirable to obtain machinery vibration data for the sensor oriented in the horizontal, vertical and axial direction. Additionally, the capture of the higher frequency stress wave activity (in at least one direction) is beneficial for detecting impacting, fatiguing and friction. The mounting of the sensor via a 2-pole magnet on a curved surface limits the ability of the sensor to detect the higher frequency stress wave activity introduced by friction due to the limited bandwidth (~5 kHz) introduced by the 2-pole magnet.

If it is deemed important to reliably detect friction at an early stage, the two pole magnet should be replaced by a flat rare earth magnet requiring a smooth flat space (such as a mounting pad) to attach the magnet. Using a flat rare earth magnet could require three mounting pads if horizontal, vertical and axial measurements were acquired at each bearing. The inconvenience of mounting three mounting pads on each bearing as well as time restraints discourages the acquisition of broadband (up to 15-20 kHz) data in the three directions.

For those cases where it is important to reliably detect friction activity (requiring broadband detection capability), the acquisition of data is generally restricted to one direction when a single axis sensor is used. An alternative to the single axis sensor with flat magnet is the use of a conventional triaxial accelerometer which requires a special mounting pad or other surface preparation. This method lacks the versatility of a 2-pole or flat magnet and hence not widely adapted in route based data acquisition programs.

The triaxial accelerometer developed by Emerson specifically for route base data acquisition has the versatility of the single axis accelerometer. When the triaxial accelerometer is placed on a curved surface, the performance of the sensor in the z direction is approximately equivalent to the single axis accelerometer attached to a 2-pole magnet placed on the curved surface. When the triaxial accelerometer is placed on a flat surface (such as a mounting pad), the performance of the sensor in the z direction is approximately equivalent to the single axis accelerometer attached to a flat surface (mounting pad). In the next section, development and laboratory verification of the triaxial accelerometer are discussed. This will be followed by a section demonstrating the applicability of the sensor to route based data acquisition programs. The last section will be conclusions.

Development of the Emerson Triax Accelerometer

The design criteria for the triaxial accelerometer are listed below.

1. Versatility of two pole magnet maintained.
2. Magnet be integral to sensor thereby avoiding sensor magnet interface.
3. Sensing in the z (x-y is plane parallel to feet) direction be flat within 3 dB up to 10 kHz.
4. Sensing in the z direction be responsive up to 25 kHz for stress wave activity with sensor mounted on flat surface (such as a mounting pad).
5. Sensing in horizontal (x-y) plane be flat within 3 dB up to 4 kHz.

A plan view of the triaxial sensor under discussion is presented in Figure 1. The sensing element for the “x” direction is always parallel to the feet as shown in Figure 1. The y-z sensing direction is shown in Figure 1. The two feet shown in Figure 1 are broader than what is normally the case for the two pole magnet used with a single axis sensor. When placed on a mounting pad, the increased area (relative to typical 2-pole magnet) between feet and mounting pad provides sufficient holding force to provide the desired sensor bandwidth in the z-direction.

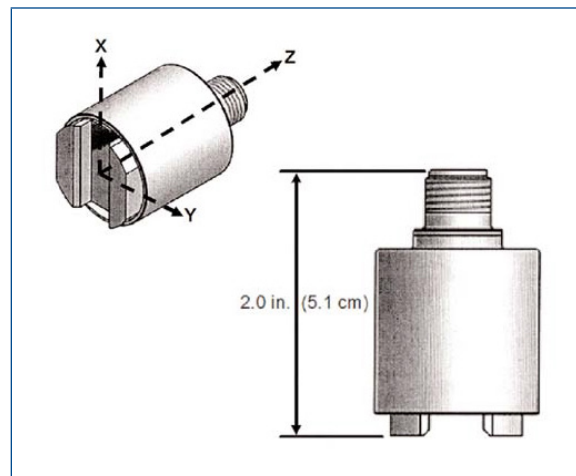


Figure 1. Plan view of the Triax Accelerometer. X-axis direction always parallel to 2-pole magnet feet.

The frequency response sweep between 100 Hz and 50,000 Hz for the triaxial accelerometer are presented in Figure 2. The resonance for this sensor is around 24 kHz showing a peak around 10 dB at resonance. There is a decrease in response in the proximity of 15 kHz. The activity around the resonance will vary somewhat between sensors, but the key points are the z-axis sensor is within 3 dB at 10 kHz and remains responsive to 30 or so kHz. A reference 50 kHz frequency response sweep for a single axis sensor on flat surface is presented in Figure 3. The response is similar to the z-direction sensor of the triaxial accelerometer in the 10 kHz to 30 kHz range.

To evaluate further the response of the triaxial accelerometer to stress wave activity over a frequency range of 6 to 25 kHz (where some impacting and most friction generated stress wave activity are expected), a stack of piezo electric disc were attached to the end of a massive steel table. The piezo electric disc stack was excited by a reasonably high voltage periodic signal. The driving periodic signal consisted of a sinusoidal signal gated on for 2 msec and then off for the remaining duration of the driving signal period (the repetition rate was about 13 times per second).

Sensors were placed on the top surface of the metal table. Two high frequency sensors were used as the reference sensors. The single axis sensor was mounted to the table surface with a flat rare earth magnet. Three integral magnet triaxial sensors were evaluated.

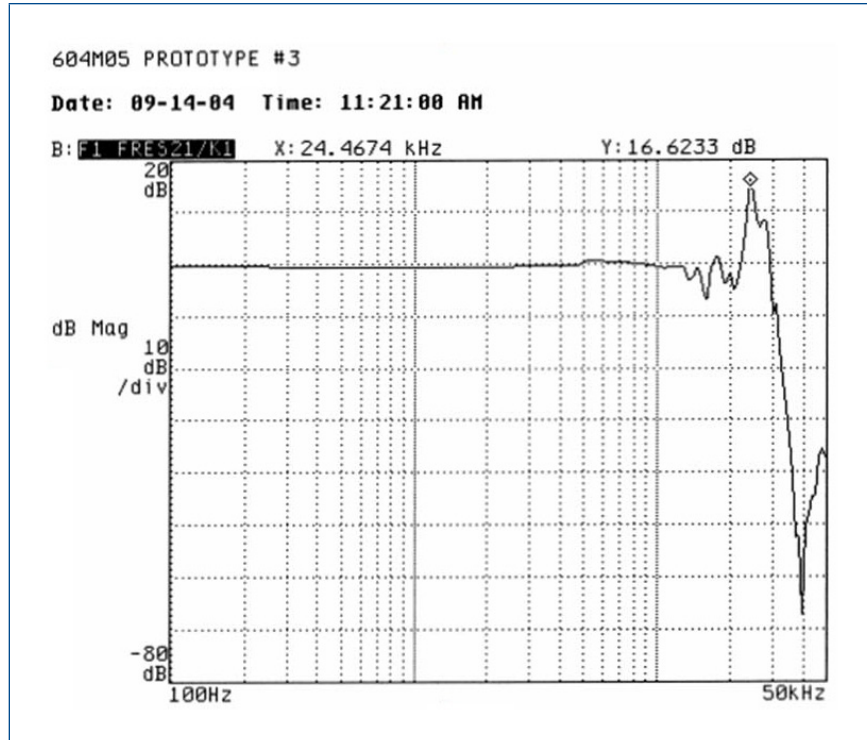


Figure 2. Frequency response sweep between 100 Hz and 50,000 for z-direction sensor in Triax accelerometer.

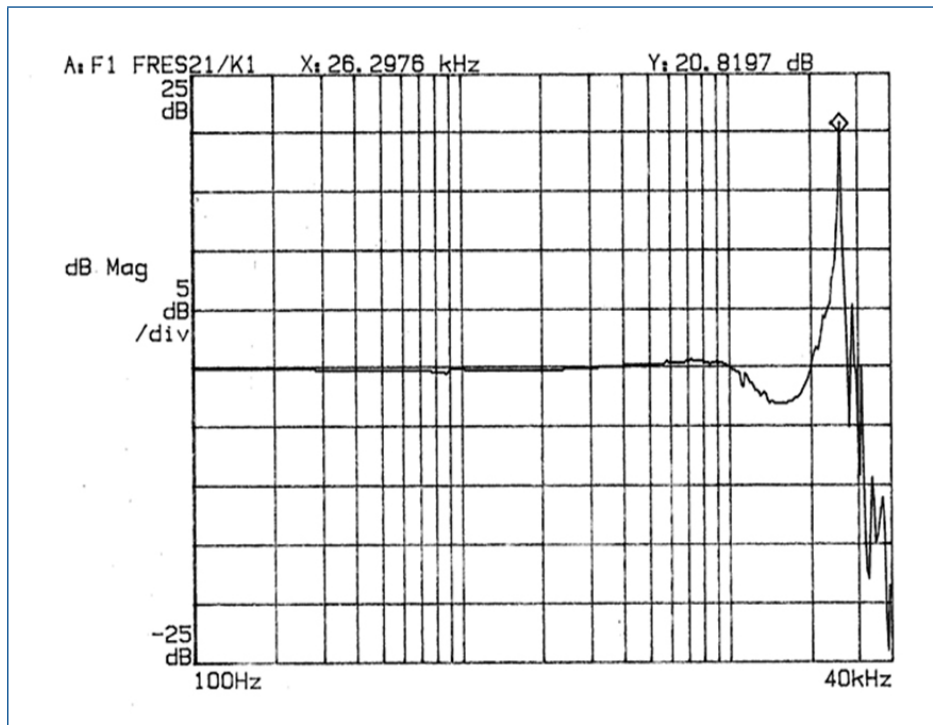


Figure 3. Frequency response between 100 Hz and 50,000 Hz for single axis accelerometer mounted on flat surface.

The PeakVue™ spectral data acquired from the reference sensor, single axis sensor, and a triaxial (z direction) sensor for the case when the excitation frequency was 25 kHz are presented in Figure 4. The PeakVue spectral response of these three sensors with a second triaxial sensor at multiple carrier frequencies is tabulated in Table 1. The key observation is the z axis triaxial sensor is capable of detecting stress wave activity beyond the 25 kHz range which is sufficient to capture stress wave generated by impacting, fatiguing, and friction when mounted on a flat surface.

Table 1. PeakVue Spectral g's for multiple sensors with multiple carrier frequencies				
Carrier frequency (kHz)	Reference sensor (g's RMS)	Triax 1 z-axis (g's RMS)	Triax 2 z-axis (g's RMS)	Single axis (g's RMS)
6	0.025	0.01	0.01	0.01
10	0.034	0.03	0.02	0.015
15	0.054	0.05	0.04	0.02
20	0.15	0.20	0.08	0.05
25	0.22	0.20	0.18	0.20

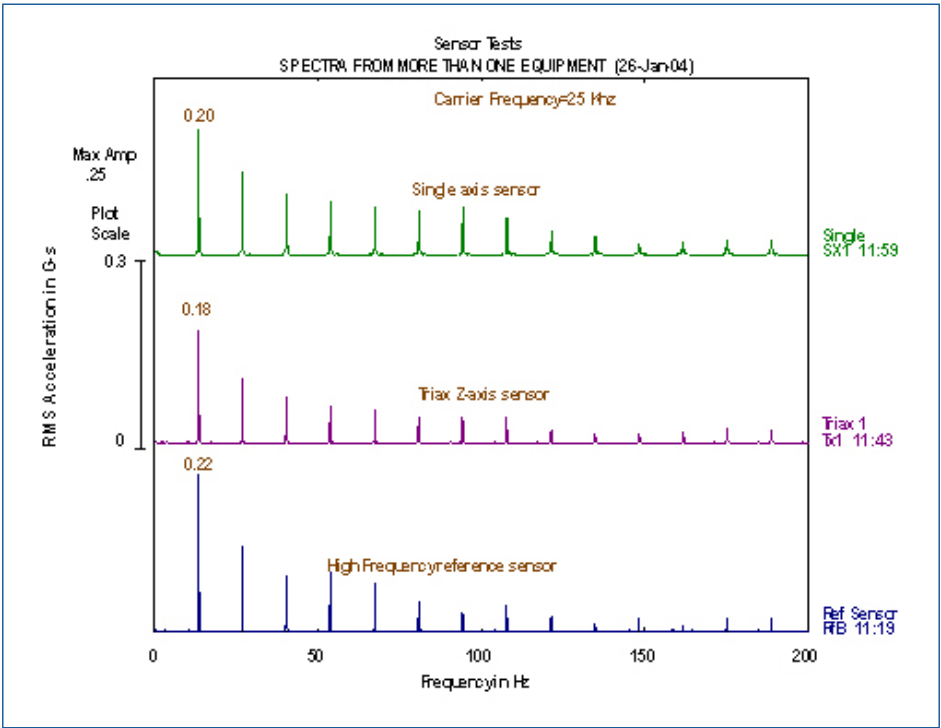


Figure 4. PeakVue response of high frequency accelerometer, z-axis of triax accelerometer and single axis accelerometer/flat rare earth magnet to an impulse excitation of 25 kHz carrier gated on 2 msec with a periodic rate of 13 per second.

Route Based Vibration Data Acquisition Using the Triaxial Sensor

In this section, comparative data are presented which was acquired from a single axis accelerometer and from the Triax accelerometer. The first set of data are for trending parameters for single axis accelerometers mounted in the horizontal, vertical and axial direction compared to the x-y-z sensors in the triax accelerometer. The second set of data are for the z-direction sensor in Axial direction over a six month time span covering the detection of a BPFI fault in velocity spectral data and subsequent propagation of fault until bearing was replaced. The third set of data is for an outer race defect (BPFO) detected employing PeakVue and single axis accelerometer. The final set of data is for an outer race fault (fluting) on an exhaust fan using PeakVue data from the triax accelerometer.

Comparison of Trending Parameter

A motor/pump machine was chosen for the enclosed trending parameter comparison (single axis versus triax accelerometer). The parameter trended are the velocity overall, 1x, 2x and 3-8x RMS values. The single axis data acquisition requires the placement at three different spots whereas the triax requires sensor placement at a single location. The single axis data was acquired on June 8, 2007 and the triax data was acquired on July 7, 2007. Both sensors were placed on curved surface for data acquisition. The acquired trend parameters are tabulated in Table 1. There is very little difference in the two data sets.

Inner Race Detected and Trended with Triax

The velocity spectral data from the z sensor of the triax sensor placed on a curved surface on a Pulverizer gearbox are presented in Figure 5 clearly showing an inner race fault. The velocity spectral data acquired over a six month period from the same triax sensor mounted on the curved surface are presented in Figure 6. The defect was first observed in the December 14, 2007 data set and increased in severity level through the January 17, 2008 data set when the bearing was replaced. A photograph of the inner race from the removed bearing is presented in Figure 7 which shows significant damage.

Table 2. Comparative trend data between three single axis readings and Triax readings

	Overall		1x		2x		3-8x	
	Triax*	Single+ Axis	Triax*	Single+ Axis	Triax*	Single+ Axis	Triax*	Single+ Axis
MOH (z)	0.102	0.107	0.077	0.077	0.063	0.069	0.024	0.024
MOV (x)	0.030	0.029	0.028	0.026	0.007	0.0090	0.0076	0.0076
MOA (y)	0.065	0.060	0.056	0.045	0.032	0.027	0.0030	0.0036
MIH (z)	0.112	0.126	0.091	0.103	0.056	0.061	0.035	0.038
MIV (x)	0.054	0.052	0.047	0.046	0.024	0.022	0.011	0.011
MIA (y)	0.072	0.070	0.047	0.047	0.054	0.039	0.0047	0.021
PIH (z)	0.207	0.200	0.200	0.193	0.0073	0.010	0.054	0.043
PIV (x)	0.112	0.097	0.063	0.080	0.013	0.010	0.091	0.038
PIA (y)	0.121	0.093	0.104	0.064	0.0072	0.013	0.042	0.042
POH (z)	0.123	0.153	0.120	0.148	0.012	0.013	0.022	0.021
POV (x)	0.128	0.135	0.124	0.130	0.013	0.012	0.028	0.024
POA (y)	0.083	0.096	0.078	0.086	0.0059	0.0065	0.025	0.015

*Triax data acquired on 7/17/07. Units (ips)

*Singular data acquired on 6/8/07. Units (ips)

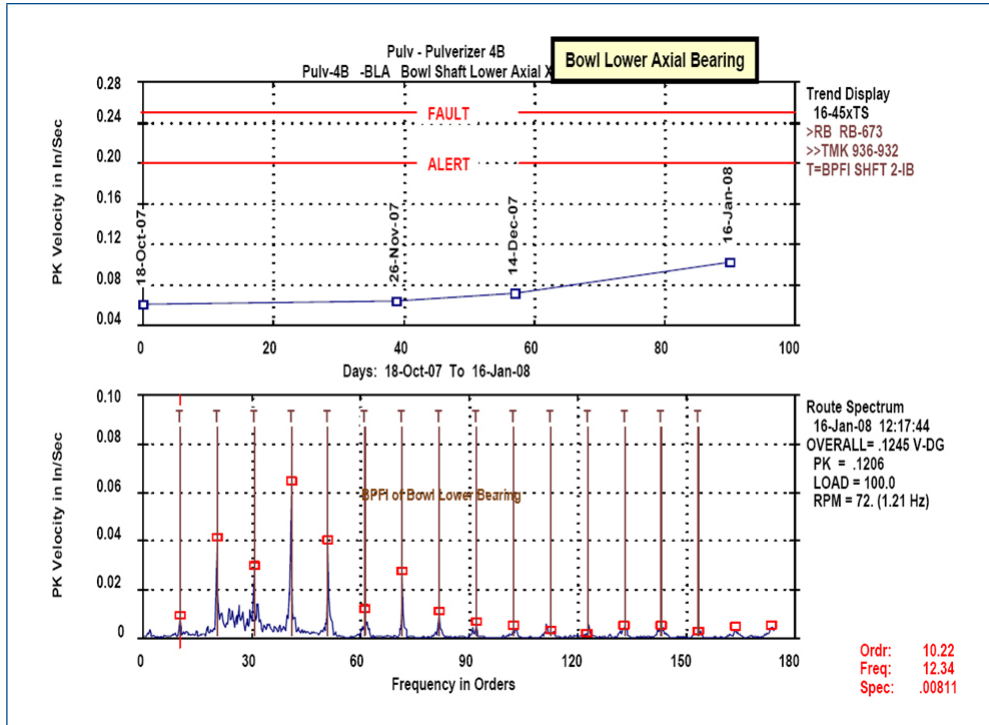


Figure 5. Velocity spectra data from z-axis sensor on Pulverizer Gearbox clearly indicating inner race bearing fault.

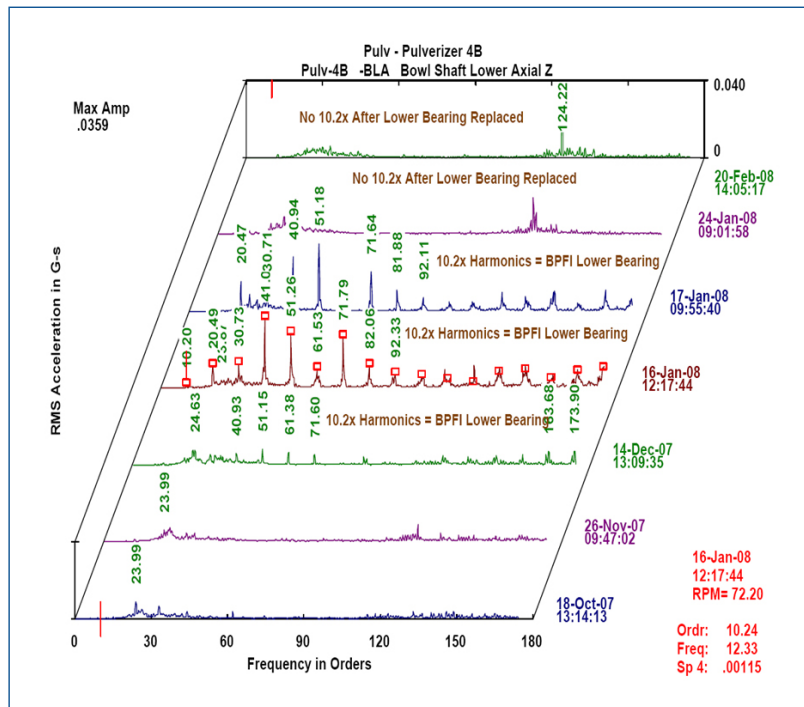


Figure 6. Water fall velocity spectral data from z-axis sensor on Pulverizer Gearbox over 6 month period with inner race fault present between December 14, 2007 and January 17, 2008 when bearing was replaced.



Figure 7. Photograph of the defective inner race from bearing removed from Pulverizer Gearbox following January 17, 2008 data set in Figure 6.

Outer Race Defect and PeakVue

An outer race defect detected on August 2, 2007 employing PeakVue from single axis accelerometer mounted on pulverizer exhaust fan is presented in Figure 8. On October 22, 2007, the triax sensor was being used for collection of route data. The PeakVue spectra from this same exhaust fan are presented in Figure 9. The outer race defect is still obvious, but with less amplitude at the defect frequency. The 1-x component has grown slightly and there are obvious side banding (amplitude modulation) of the BPFO fault activity with the running speed suggesting possible unbalance may be increasing.

PeakVue Trend and Spectra around Nearing Replacement

PeakVue spectra from the z sensor in triax accelerometer are presented in Figure 10 from pulverizer exhaust fan clearly showing BPFO fault. The peak g-level trend data from the PeakVue waveform are presented in Figure 11 over a 5+ month period. The bearing was replaced near March 4, 2008 showing significant decrease in the peak g-level amplitude. A photograph of the defective bearing (showing fluting) is presented in Figure 12.

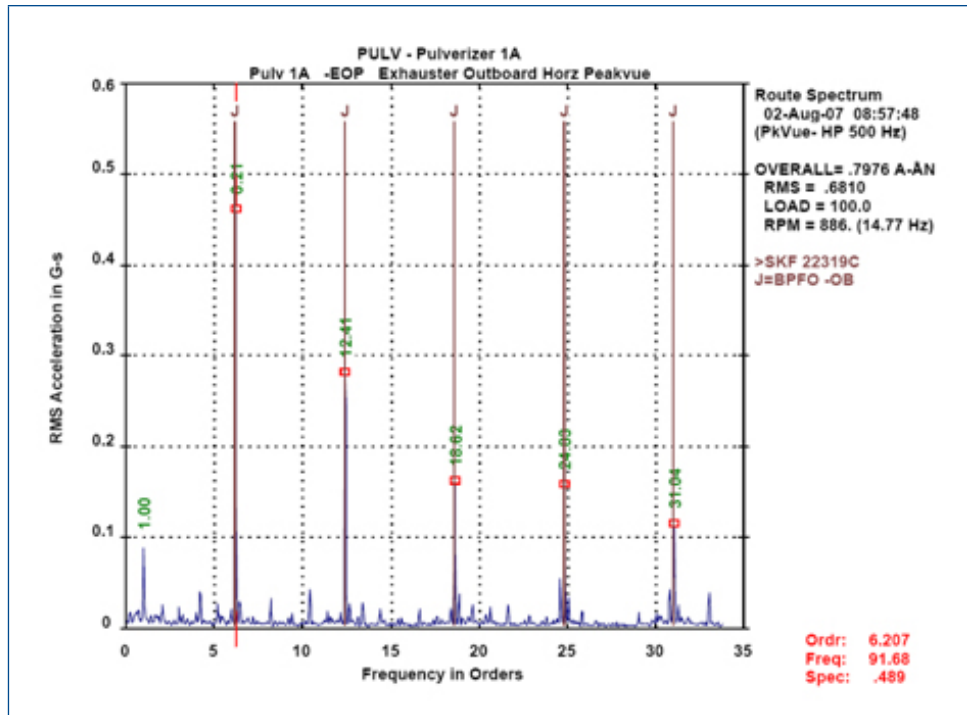


Figure 8. BPFO fault detected August 2, 2007 with PeakVue from Single Axis Accelerometer. Note slight amplitude modulation at tuning speed.

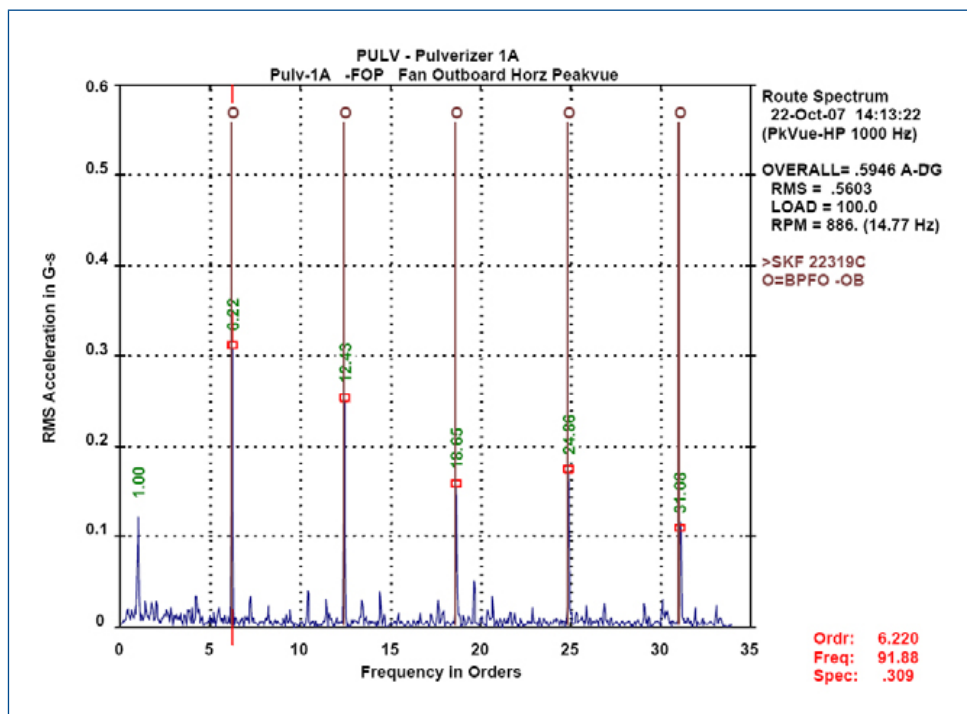


Figure 9. BPFO at same acquisition point of Figure 8 using Triax z-axis accelerometer on October 22, 2007. Note amplitude modulation has increased slightly relative to data in Figure 8.

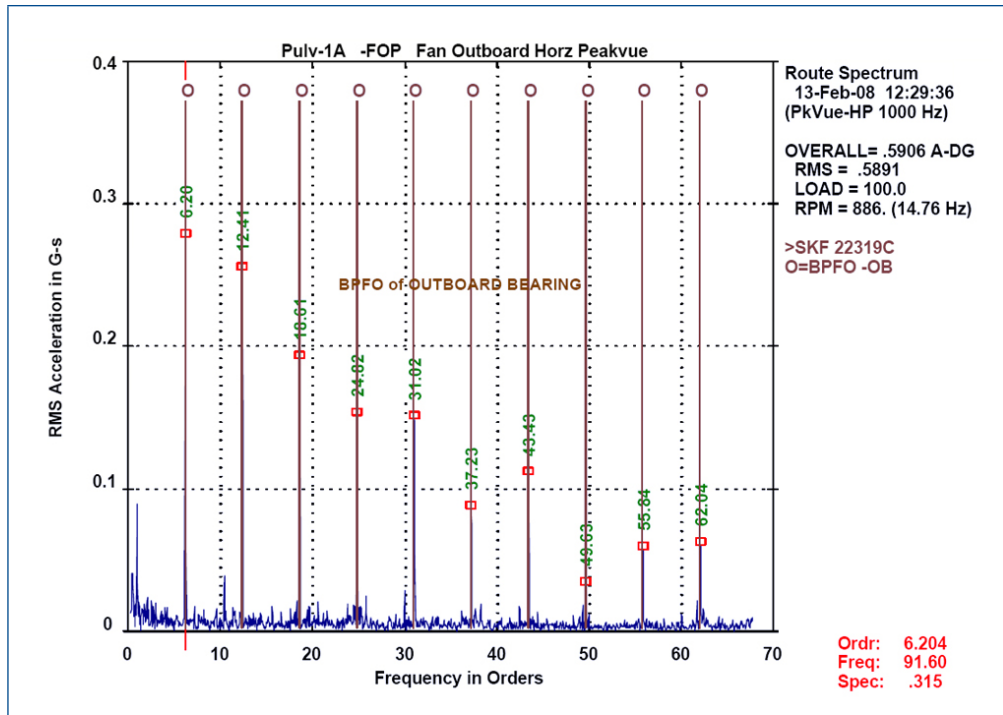


Figure 10. Z-axis PeakVue data from pulverizer exhaust fan on February 13, 2008 showing an outer race defect.

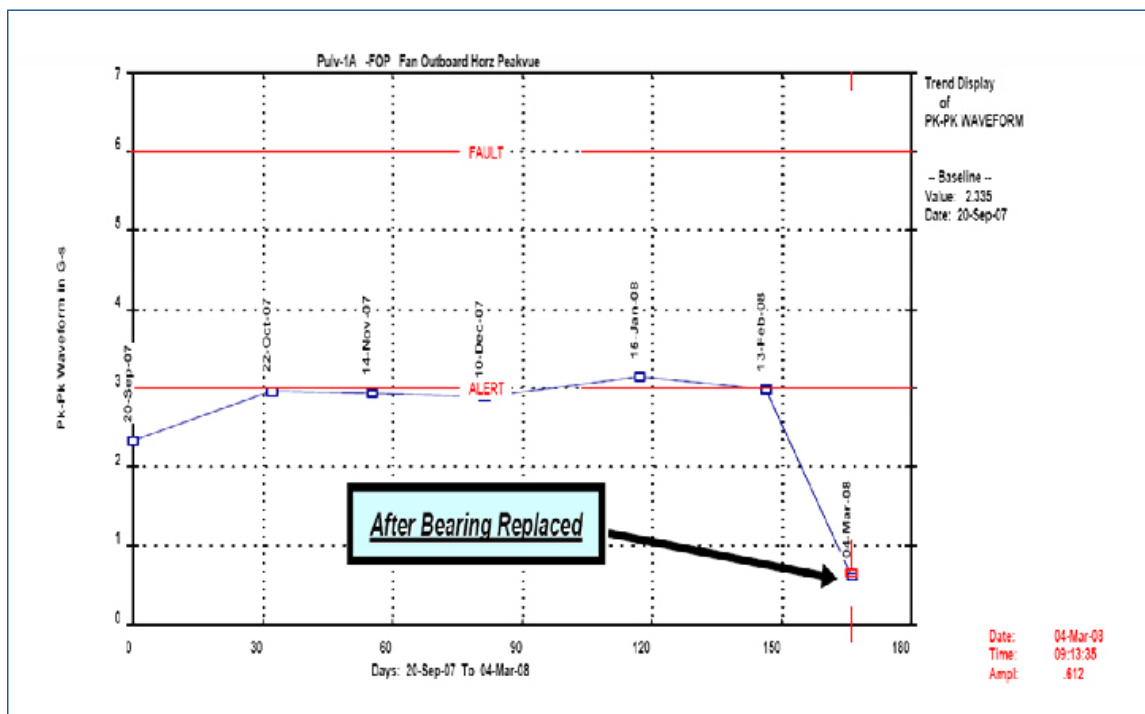


Figure 11. Peak g-level PeakVue trend data from z-axis sensor over 5.5 month period from same measurement point from which PeakVue spectra data in Figure 10 acquired.



Figure 12. Defective bearing (fluting) from Pulverizer exhaust fan where data presented in Figures 10 and 11 were acquired.

Conclusion

The primary objective in the development of the triax sensor was to have an equivalent sensor in the z (typically in vertical) direction to the commonly used single axis accelerometer when on a curved surface. Additionally, the x-y sensors can be used where x generally is axial and y is horizontal (assuming z is vertical). The triax sensor was proven to meet the design objectives in the laboratory followed by application in the field. If the triax sensor is placed on a smooth flat magnetic surface, the bandwidth of the z sensor is increased to the 25-30 kHz range which is adequate for high frequency stress wave activity accompanying friction, fatiguing and fluting. Use of the triax sensor in the route mode of data collection in the field has reduced data collection time on an average of 30%.

The Emerson logo is a trademark and service mark of Emerson Electric Co. The AMS logo is a mark of one of the Emerson family of companies. All other marks are the property of their respective owners.

The contents of this publication are presented for informational purposes only, and while every effort has been made to ensure their accuracy, they are not to be construed as warranties or guarantees, express or implied, regarding the products or services described herein or their use or applicability. All sales are governed by our terms and conditions, which are available on request. We reserve the right to modify or improve the designs or specifications of our products at any time without notice.

Emerson
Reliability Solutions
835 Innovation Drive
Knoxville, TN 37932 USA
☎ +1 865 675 2400
🌐 www.emerson.com/ams

